ARTICLE OPEN

Check for updates

Senescent lung fibroblasts in idiopathic pulmonary fibrosis facilitate non-small cell lung cancer progression by secreting exosomal MMP1

Yuqiong Lei[1], Cheng Zhong[1], Jingyuan Zhang[1], Qi Zheng[1], Yongle Xu[1], Zhoubin Li[2]✉, Chenwen Huang[1,3]✉ and Tao Ren[1,4]✉

Lung cancer is a fatal complication of idiopathic pulmonary fibrosis (IPF) with a poor prognosis. Current treatments are insufficient in improving the prognosis of lung cancer patients with comorbid idiopathic pulmonary fibrosis (IPF-LC). Senescent fibroblasts, as stromal cells in the tumor microenvironment, influence tumor progression via exosomes. With evidence that fibroblast senescence is an important mechanism of IPF, we investigated the impact of senescent IPF lung fibroblast (diseased human lung fibroblasts, DHLF)-derived exosomes on non-small cell lung cancer (NSCLC). We found DHLF expressed significant senescence markers, and promoted NSCLC proliferation, invasion, and epithelial-mesenchymal transition. Specifically, senescent DHLF showed strong secretion of exosomes, and these exosomes enhanced the proliferation and colony-forming ability of cancer cells. Proteomic analysis showed DHLF-derived exosomes exhibited upregulated senescence-associated secretory phenotype (SASP) factors, notably MMP1, which activates the surface receptor PAR1. Knocking down MMP1 or using PAR1 inhibitors reduced the tumor-promoting effects of DHLF-derived exosomes in vivo and in vitro. Mechanistically, MMP1 acted by activating the PI3K-AKT-mTOR pathway. In conclusion, our results suggest that exosomal MMP1 derived from senescent IPF fibroblasts promotes NSCLC proliferation and colony formation by targeting PAR1 and activating the PI3K-AKT-mTOR pathway. These findings provide a novel therapeutic approach for patients with IPF-LC.

Oncogene (2025) 44:769–781; https://doi.org/10.1038/s41388-024-03236-5

INTRODUCTION

Idiopathic pulmonary fibrosis (IPF) is a progressive interstitial lung disease associated with aging and an independent risk factor for lung cancer. Epidemiological studies indicate that 3–22% of patients with IPF develop lung cancer during follow-up [1], with the cumulative incidence increasing over time, making lung cancer a primary cause of mortality in these patients [2]. Research has revealed that IPF combined with lung cancer (IPF-LC) exhibits higher invasiveness compared to sporadic lung cancer [3].Non-small cell lung cancer (NSCLC), which includes squamous cell carcinoma and adenocarcinoma, is the main pathological type of IPF-LC. Currently, there are no specific treatment guidelines for IPF-LC. Standard lung cancer therapies such as chemotherapy, radiotherapy, immunotherapy, and targeted therapy have been found to cause acute exacerbations of IPF in clinical practice [4, 5], thereby limiting treatment options for patients with IPF-LC. Elucidating the molecular mechanisms underlying IPF-LC progression is crucial for developing new therapeutic targets.

IPF-LC tumors are commonly located in the peripheral or lower lobes of the lungs, regions affected by fibrosis, suggesting a link between fibrosis and lung cancer development. Cancer-associated fibroblasts (CAFs), a prominent cell population in the tumor microenvironment (TME), have garnered significant attention in recent years [6]. CAFs promote tumor cell proliferation, immune evasion, metastasis, and therapeutic resistance by remodeling the ECM and secreting growth factors and cytokines. Notably, studies have found many similarities between myofibroblasts in IPF and CAFs [7]. Both exhibit sustained overactivation and abnormal proliferation, mesenchymal characteristics, heterogeneous phenotypes, and similar signaling pathway activations. And fibroblasts in IPF were found to promote tumorigenesis and progression [8, 9]. However, the quantity of available studies is limited.

Cellular senescence, an irreversible process leading to cell cycle arrest, has been increasingly implicated in IPF pathogenesis [10]. In cancer research, senescence was initially considered a tumor-suppressive mechanism; however, it has been recently described as a double-edged sword [11]. Studies have shown that senescent fibroblasts can induce abnormal proliferation of various precancerous cells, leading to tumor formation and promoting cancer cell invasion and migration [12–14]. In IPF-LC, the potential role of senescent fibroblasts in promoting the malignant behavior of NSCLC cells warrants investigation. Senescence-associated secretory phenotype (SASP) refers to the specific secretory profile of senescent cells, involving the selective overexpression of

[1]Department of Respiratory Medicine, Shanghai Sixth People's Hospital Affiliated to Shanghai Jiao Tong University School of Medicine, Shanghai 200233, China. [2]Department of Lung Transplantation and Thoracic Surgery, First Affiliated Hospital, School of Medicine, Zhejiang University, Hangzhou 310003, China. [3]Department of Clinical Research Centre, Shanghai Sixth People's Hospital Affiliated to Shanghai Jiao Tong University School of Medicine, Shanghai 200233, China. [4]Stem Cell Center, Shanghai Sixth People's Hospital, Shanghai 200233, China. ✉email: 1510023@zju.edu.cn; 442127683@qq.com; liuyuanrentao@sjtu.edu.cn

Received: 11 July 2024 Revised: 13 November 2024 Accepted: 18 November 2024
Published online: 11 December 2024

numerous factors, predominantly interleukin-6 (IL-6), interleukin-8 (IL-8), CXC motif chemokine ligand 1 (CXCL1), and various matrix metalloproteinases (MMPs) [15]. Extracellular vesicles (EVs), which are known to be key mediators of intercellular communication, are significant components of the SASP [16, 17].

The role of senescent fibroblasts in promoting tumor cells has been a prominent research focus. IPF is an aging-associated disease with fibroblast senescence recognized as its key pathological feature. Therefore, understanding the impact and potential mechanisms of fibroblast senescence on IPF-LC is crucial. In this study, we aim to investigate the senescence characteristics of primary lung fibroblasts obtained from patients with IPF and elucidate, for the first time, the SASP factors profile of exosomes secreted by these fibroblasts and their promotive effects on NSCLC.

RESULT

Reduced proliferative capacity and enhanced senescence traits are observed in fibroblasts from patients with IPF

To investigate cellular senescence in IPF lung cells, we implemented immunofluorescence co-localization on lung specimens from IPF patients, assessing senescence markers (γH2AX, p53, p16, p21) in RAGE+ (AT1), SPC+ (AT2), and Vimentin+ (fibroblast) cells. As shown in Fig. 1A, B and Supplementary Fig. 1B, all three cell types exhibited senescent phenotypes, with fibroblasts comprising the largest fraction, followed by AT2 cells. A comparison between IPF and healthy controls revealed elevated γH2AX, p53, p16, and p21 expression in IPF lung tissues (Fig. 1C, D).

Primary fibroblasts were extracted from specimens, revealing that IPF fibroblasts (DHLFs) exhibited hallmark senescence features, such as increased cell size and irregular morphology (Supplementary Fig. 1C). DHLFs also showed higher expression of α-SMA and Vimentin compared to normal fibroblasts (NHLFs) (Fig. 1E, F, Supplementary Fig. 1D, E). Proliferation assays (Ki67 and EdU) indicated that DHLFs had about half the proliferation capacity of NHLFs (Fig. 1E, F). Elevated p16 and p21 levels were confirmed by immunofluorescence and western blot (Fig. 1E–G, Supplementary Fig. 1E). SA-β-Gal activity assays further confirmed senescence, with 30% of DHLFs testing positive compared to 10% in NHLFs at passage 3 (P3) (Fig. 1H, I).

Collectively, these experiments validated that IPF fibroblasts exhibit significantly reduced proliferative capacity and pronounced senescent characteristics.

Role of senescent IPF fibroblasts in promoting NSCLC proliferation and invasion

Senescent CAFs have been demonstrated to enhance the proliferative and metastatic capacities of cells. Building on this knowledge, our study aimed to explore whether senescent IPF fibroblasts influence the proliferation, migration, and invasion of NSCLC cells. We used transwell chambers to create an indirect co-culture model (Fig. 2A) and conducted functional assays on A549 and SK-MES-1 cells following co-culture. NSCLC cell lines co-cultured with IPF fibroblasts exhibited a morphological transformation from a cobblestone-like appearance to an elongated spindle shape (Fig. 2B). This morphological shift was indicative of epithelial-mesenchymal transition (EMT). Subsequent CCK8 assays revealed that A549 and SK-MES-1 cells co-cultured with IPF fibroblasts exhibited increased proliferative capacity (Fig. 2C, D). Additionally, lung cancer cells co-cultured with IPF fibroblasts showed a significant increase in clone-formation capacity (Fig. 2E, F). Furthermore, transwell assays confirmed that A549 and SK-MES-1 cells co-cultured with IPF fibroblasts exhibited significantly enhanced invasive and migratory capabilities, particularly in the A549 cell line (Fig. 2G–J). To further elucidate the role of EMT in these changes, we analyzed the expression of EMT-related proteins in both groups. Our results indicated a reduction in the epithelial marker, E-cadherin, and an increase in the mesenchymal markers, N-cadherin, Vimentin and Snail in the DHLF group (Fig. 2K–M), suggesting that IPF fibroblasts actively promoted EMT in NSCLC. These findings demonstrate that senescent IPF fibroblasts contribute to the increased malignancy of NSCLC cells by promoting proliferation, EMT, and invasion.

Exosomes from IPF fibroblasts promote malignant transformation in NSCLC in vitro

To further identify the specific secretory components released by IPF fibroblasts that facilitate phenotypic alterations in NSCLC, we separately isolated microvesicles (MVs), exosomes (Exos) and extracellular vesicle-free (EVs-free) supernatant from serum-free conditioned media (Fig. 3A). Western blot analysis was conducted to detect the expression of the microvesicle marker (Annexin V) and the exosome markers (CD9 and CD63) to confirm successful extraction (Fig. 3B). Subsequently, we co-incubated lung cancer cells with MVs, Exos, or EVs-free supernatants secreted by the same number of cells and then used CCK8 and colony formation assays to evaluate the effects of different supernatant components on the proliferation and colony-forming abilities of lung cancer cells. The results showed that exosomes exhibited the most significant pro-tumor effect, followed by vesicle-free supernatant, with microvesicles having the weakest effect (Fig. 3C–F). Exosomes have emerged as a crucial mechanism of intercellular communication, garnering significant attention for their roles in various physiological and pathological processes. Electron microscopy revealed that the exosomes exhibited the characteristic bilayer vesicular structure, and NTA confirmed that the exosome sizes ranged from 30 to 150 nm (Fig. 3G, H). Notably, IPF fibroblasts secreted significantly more exosomes than normal fibroblasts, with higher protein content (Supplementary Fig. 2B, C). Fluorescently labeled exosomes (green) were observed to be internalized by NSCLC cells within 4 h, with substantial uptake by 24 h (Fig. 3I).

For assessing the proliferative and clonogenic changes following exosome uptake, we incubated A549 and SK-MES-1 cells with 20 μg/ml of exosomes. NSCLC cell lines that internalized exosomes exhibited enhanced proliferation, with IPF-derived exosomes (DHLF-exosome) showing a significantly stronger growth-promoting effect than NHLF-exosome (Fig. 3J, K). Additionally, DHLF-exosomes significantly enhanced the clonogenic potential of both A549 and SK-MES-1 cells (Fig. 3L, M). These findings suggest that exosomes released by IPF lung fibroblasts significantly enhance the malignant phenotype of NSCLC cells.

Upregulated proteins in DHLF-exosomes highlight SASP factors linked to NSCLC progression

To identify exosomal components with potential pro-tumorigenic roles, we conducted a proteomic analysis of exosomes. Mass spectrometry revealed that DHLF-exosomes exhibited an upregulation of 392 proteins compared to NHLF-exosomes. These proteins included key components of SASP, such as *FBLN2, IL-6, MMP1, MMP3*, and *IGFBP3* (Fig. 4A). The top 10 highly expressed proteins in exosomes secreted by IPF fibroblasts included *POSTN*, *CYGB*, *SLC22A4*, *GASK1B*, *SERPINE2*, *C7*, *TNFAIP6*, *SNRPD1*, *SELENOP*, and *XPO1*. Gene Ontology (GO) enrichment analysis showed that the term 'extracellular exosome' (GO:0070062) was the most enriched cellular component, corroborating the enhanced exosomal secretion capacity of IPF fibroblasts (Fig. 4B). The PI3K-AKT-mTOR signaling pathway was one of the most enriched KEGG pathways, with the cellular senescence pathway also prominently represented (Fig. 4C). Additionally, several senescence-associated pathways were enriched, including ferroptosis, the p53 pathway, and autophagy, they are expected to be important mechanisms of senescence in IPF lung fibroblasts.

To further predict potential aging pathways, we analyzed single-cell sequencing data from NHLF and DHLF (Supplementary Fig. 3). Approximately 33372 fibroblasts met the quality

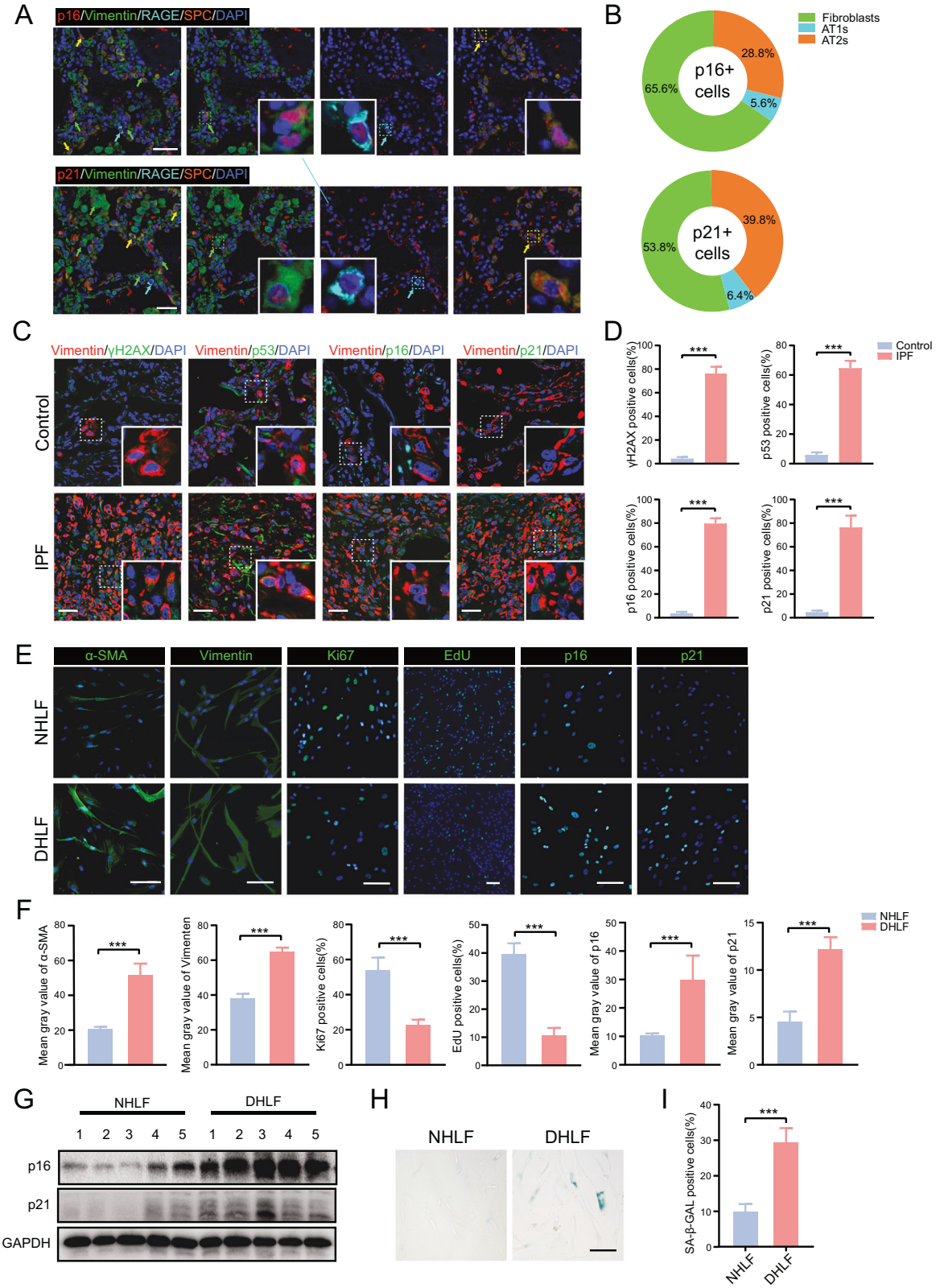

control criteria, and six fibroblast clusters were identified using unsupervised clustering with the Scanpy (v1.8.2) package (Supplementary Fig. 3A, B). Among them, clusters 5 and 6 showed a significantly higher proportion in the DHLF group (Supplementary Fig. 3C), suggesting that these two subclusters are IPF-specific fibroblast subtypes. Using an aging gene set to analyze the cellular senescence levels of different cell subclusters [18], we found that cluster 6 had significantly higher senescence scores than other subclusters(Supplementary Fig. 3E, F). Further analysis revealed that cluster 6 cells were enriched not only with

Fig. 1 Comparative assessment of proliferative and senescent characteristics of IPF Fibroblasts. A, **B** Co-localization of senescence markers (p16, p21) with RAGE (AT1), SPC (AT2), and Vimentin (fibroblast) via immunofluorescence. Representative images are shown in (**A**). Distribution of p16+ cells and p21+ cells across three different cell types was displayed through pie charts (**B**). Scale bar, 50 μm. **C**, **D** Immunofluorescence detection of the DNA damage marker (γ-H2AX) and senescence markers (p53, p16, and p21) in control and IPF lung tissues. Representative images acquired via confocal immunofluorescence and the positive expression rate are shown in (**C**) and (**D**), respectively. Scale bar, 50 μm. **E**, **F** α-SMA, Vimentin, Ki67, p16, and p21 expression in normal human lung fibroblasts (NHLF) and diseased human lung fibroblasts (DHLF) measured by immunofluorescence. EdU assay was measured to assess cell proliferative ability. Representative images and statistical analyses are shown in (**E**) and (**F**), respectively. Scale bar, 200 μm. **G** Immunoblotting analysis showing elevated protein levels of the senescence markers p16 and p21 in DHLF compared to NHLF. **H**, **I** Increased β-galactosidase staining in DHLFs, indicating higher senescence. Scale bar, 200 μm. (Results are presented as means ± SD, $n = 5$, $^{*}p < 0.05$; $^{**}p < 0.01$; $^{***}p < 0.001$).

proteins related to extracellular matrix (ECM) remodeling and fibrosis, such as *POSTN, COL3A1, SERPINE2, CCDC80, SPARC*, and *COL1A1*, but also with several proteins associated with cellular senescence, including *IGFBP3, IGFBP7, LOX, CYP1B1*, and *EFEMP1*. *IGFBP3* has been identified as a marker of senescence in numerous studies [19]. Therefore, we used flow cytometry to separate $IGFBP3^{high}$ DHLF from $IGFBP3^{low}$ DHLF and found that $IGFBP3^{high}$ DHLF exhibited more pronounced senescence. Enrichment analysis of the highly expressed proteins in cluster 6 revealed that many aging-related pathways were significantly enriched, including Ferroptosis, the PI3K-AKT signaling pathway, and the TNF signaling pathway.

Furthermore, we conducted a quantitative assessment of SASP factors in exosomes using a list from SASPAtlas (www.SASPAtlas.com). The heatmap showed a marked increase in the expression of SASP factors within IPF exosomes (Fig. 4D). To validate the expression of fibroblast-derived SASP factors, we assessed the mRNA encoding SASP factors of *IL6*, *MMP1*, *MMP3*, *FBLN2*, *IGFBP3*, and *IGFBP4* in both NHLFs and DHLFs. All showed significant differences, with MMP1 exhibiting the most pronounced variance (Fig. 4E).

Previous studies have demonstrated that MMP1 is highly expressed in certain lung cancer cells [20]. An analysis of survival data from 482 patients with NSCLC in the Cancer Genome Atlas (TCGA) database revealed that high MMP1 expression correlates with shorter overall survival (OS) ($p = 0.013$) (Fig. 4F). Based on these findings, we hypothesize that MMP1 is a crucial SASP exosomal component secreted by IPF fibroblasts, potentially promoting NSCLC progression.

MMP1 is a key factor in DHLF-exosome-mediated progression of NSCLC

Previous studies have demonstrated that MMP1 critically impacts the active state of cancer cells [21]. Our preliminary research revealed that exosomes secreted by DHLF exhibit high levels of MMP1 expression, whereas those secreted by NHLF exhibit low levels (Fig. 4E). To further investigate whether MMP1 is a key factor in promoting cancer within the exosomes secreted by DHLF, we conducted the following experiments.

We initially assessed the expression of MMP1 in fibrotic lung tissues of patients with IPF. Co-localization of Vimentin and MMP1 in Immunofluorescence revealed that fibroblasts in IPF lungs exhibited high MMP1 expression, whereas fibroblasts in normal lung tissues showed minimal expression (Fig. 5A, B). In IPF-LC lungs, we observed the presence of multiple fibroblast foci (marked with Vimentin and annotated by "red" arrowheads) in the tumor region where MMP1 was highly expressed (Fig. 5C). Additionally, many fibroblasts were identified in the peritumoral tissues at the "tumor-fibrosis" junction, with similarly high expression of MMP1 (annotated by "green" arrowheads). IF staining of primary fibroblasts demonstrated that MMP1 expression in DHLF was significantly higher than in NHLF (Fig. 5D, E). WB analysis of cell and exosome lysates from NHLF and DHLF indicated elevated MMP1 expression in both DHLF and DHLF-exosomes (Fig. 5F). Further analysis through ELISA demonstrated that exosomes contained significantly higher concentrations of MMP1 compared to free MMP1 in the supernatant (Supplementary Fig. 2D). To further elucidate the relationship between MMP1 and cellular senescence, we examined MMP1 expression in IPF fibroblasts and their secreted exosomes across different passage numbers. Our results indicated that as fibroblasts underwent cellular senescence during several passages, MMP1 expression markedly increased (Fig. 5G).

To further confirm that MMP1 in exosomes from senescent IPF lung fibroblasts promoted tumor cell proliferation and stemness, we transfected DHLF with shCtrl and shMMP1 lentiviruses and confirmed the knockdown efficiency by WB (Fig. 5H). Exosomes were extracted using the same method (shCtrl-exo *vs.* shMMP1-exo), and co-culture experiments revealed that A549 and SK-MES-1 cells incubated with shMMP1-exo exhibited reduced proliferation and colony formation compared to those incubated with shCtrl-exo (Fig. 5I–L). These findings strongly suggest that MMP1 is a crucial factor in the DHLF-exosome-mediated promotion of NSCLC cell proliferation.

DHLF-exosome promotes lung cancer cell proliferation via PAR1-mediated PI3K-AKT-mTOR pathway activation

PAR1 is a widely recognized receptor for MMP1, extensively expressed in lung cancer cells. When activated, PAR1 promotes tumor cell growth and invasion [22]. To verify whether MMP1 exerts its pro-tumor effects through binding to PAR1, we employed the PAR1 antagonist SCH79797 (0.2 μM) and demonstrated that the pro-tumor effects of MMP1 could be inhibited by the antagonist (Fig. 6A–D). To explore how MMP1 exerts its effects after binding to PAR1, we performed RNA-seq analysis on SK-MES-1 cells incubated with and without DHLF-exosomes and identified 407 and 182 genes that were upregulated and downregulated, respectively (Supplementary Fig. 2A, B). GO analysis of differentially expressed genes showed enrichment in several pro-tumor biological processes, including positive regulation of development (GO:0051094), negative regulation of epithelial cell apoptosis (GO:1904036), and positive regulation of cell migration (GO:0030335) (Supplementary Fig. 4C, D). KEGG analysis indicated enrichment in multiple signaling pathways, including ECM-receptor interaction and PI3K-AKT signaling pathway (Fig. 6E). We also used the TCGA database to explore the correlation between the top 20 enriched signaling pathways and MMP1 expression (Supplementary Fig. 2E). The four pathways with the strongest correlations were ECM-receptor interaction ($R = 0.32$), focal adhesion ($R = 0.2$), PI3K-AKT signaling pathway ($R = 0.27$), and purine metabolism ($R = 0.22$) (Fig. 6F). This indicated a strong correlation between the PI3K-AKT signaling pathway and MMP1. To validate this finding, we detected the expression of PI3K-AKT-mTOR pathway-related proteins in A549 and SK-MES-1 cells after exosome incubation. We found that p-PI3K, p-AKT, and p-mTOR expression increased in NSCLC cells incubated with DHLF-exosomes compared to Ctrl and NHLF-exosome groups, while total protein levels remained unchanged (Fig. 6G, H). Additionally, incubation with exosomes extracted from shMMP1-DHLF weakened the activation of the PI3K-AKT-mTOR signaling pathway (Fig. 6I, J).

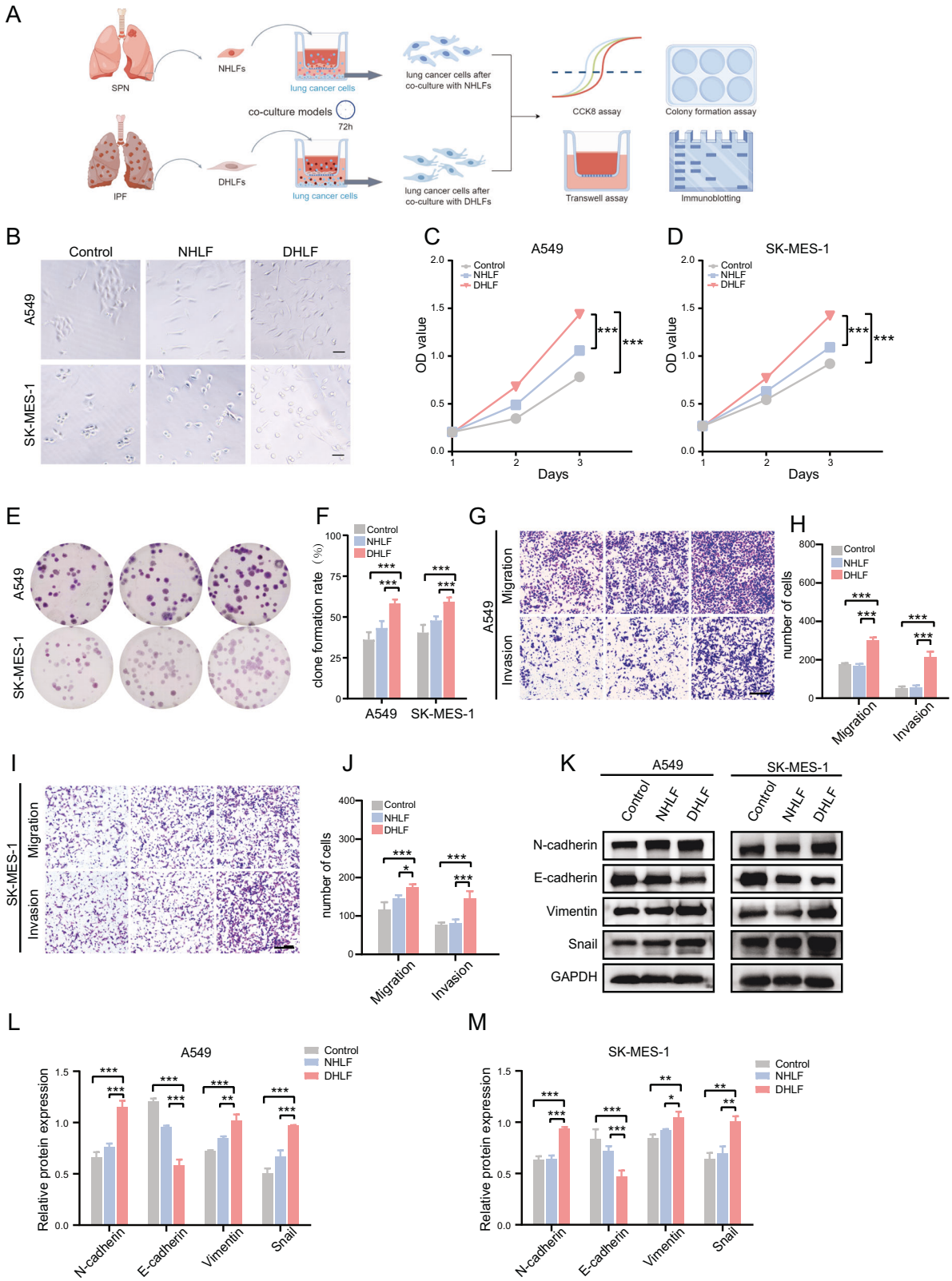

Fig. 2 IPF fibroblasts significantly enhanced the aggressiveness of NSCLC cells in vitro. A A schematic diagram illustrating the co-culture model. (Created with Figdraw). **B** Morphological changes of A549 and SK-MES-1 cells following co-cultivation with normal human lung fibroblasts (NHLFs) and diseased human lung fibroblasts (DHLFs). Scale bar, 100 μm. **C**, **D** Cellular proliferation of A549 (**C**) and SK-MES-1 (**D**) after co-culture with NHLFs and DHLFs measured by CCK8 assay. **E**, **F** Colony formation assays assessing clonogenicity of A549 and SK-MES-1 cells after co-culture with NHLFs or DHLFs. **G**–**J** Transwell assays evaluating migration and invasion abilities of A549 (**G**, **H**) and SK-MES-1 (**I**, **J**) cells after co-culture. Scale bar, 100 μm. **K**–**M** Immunoblotting analysis of EMT markers (E-cadherin, N-cadherin, Vimentin, and Snail). Representative blots shown in (**K**), with statistical analysis plots of protein levels in (**L**) and (**M**). (Results are presented as means ± SD, $n = 5$, $^{*}p < 0.05$; $^{**}p < 0.01$; $^{***}p < 0.001$).

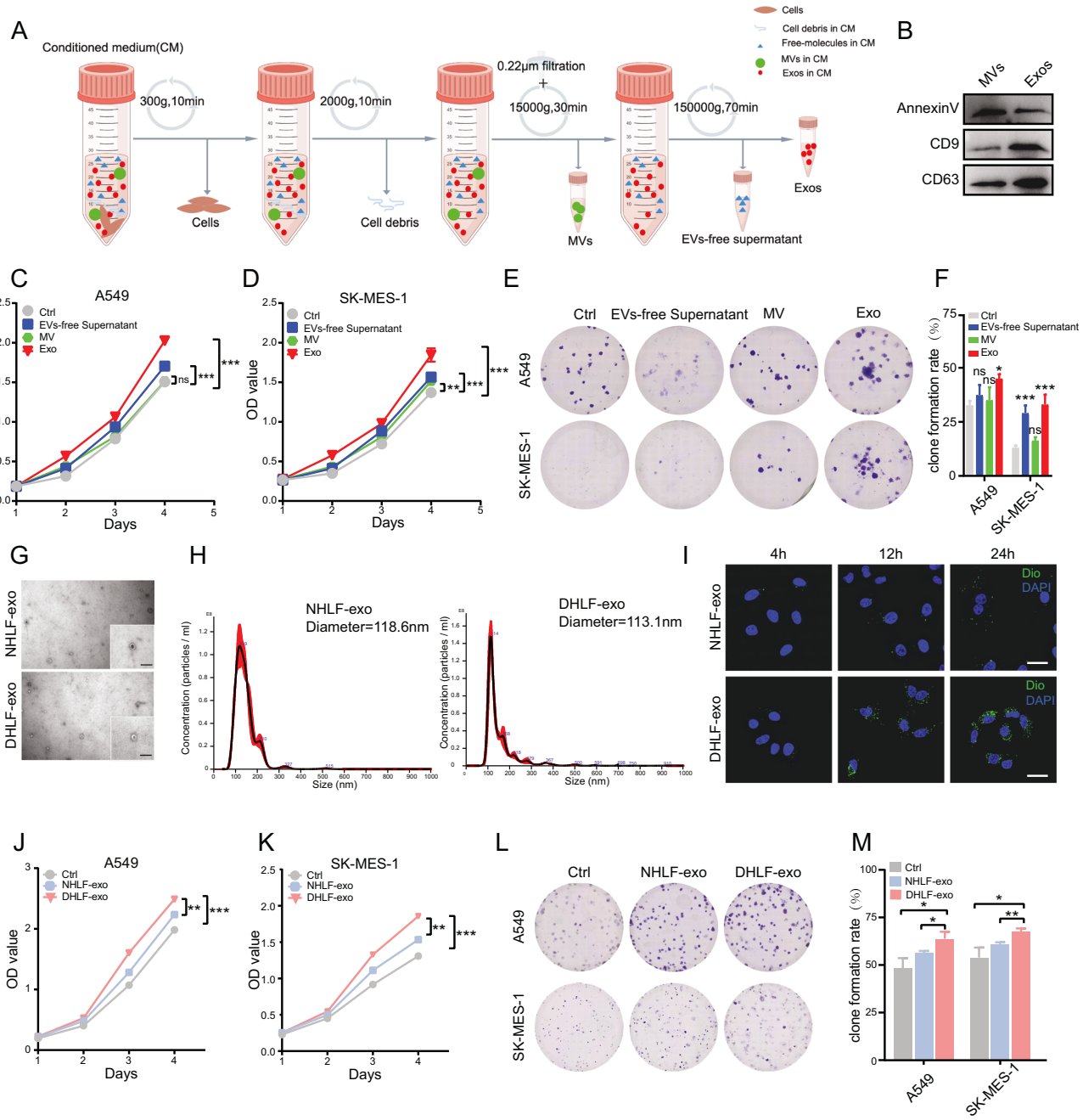

Fig. 3 Exosomes from IPF fibroblasts promote NSCLC cell proliferation. A A schematic diagram illustrating the differential ultracentrifugation process for isolating supernatant components. (Created with Figdraw). **B** Western blot analysis detecting Annexin V (microvesicle marker) and CD9, CD63 (exosome markers), confirming successful extraction. **C**, **D** The CCK8 assay assessing proliferation of A549 (**C**) and SK-MES-1 (**D**) after incubation with various supernatant components, including exosomes, microvesicles, and EVs-free supernatant. **E**, **F** Colony formation assays evaluating the colony-forming ability of lung cancer cells incubated with exosomes, microvesicles, or EVs-free supernatant. **G** TEM images of exosomes secreted by normal human lung fibroblasts (NHLF) and diseased human lung fibroblasts (DHLF). Scale bar, 100 nm. **H** Size distribution of exosomes measured via nanoparticle tracking analysis. **I** Fluorescent DiO-labeled exosomes (green) confirming internalization by recipient cells. Scale bar, 50 μm. **J**, **K** CCK8 assays evaluating A549 cells (**J**) and SK-MES-1 cells (**K**) proliferation following incubation with NHLF- and DHLF-derived exosomes. **L**, **M** Representative images (**L**) and histogram analysis (**M**) of colony formation after exosome incubation. (Results are presented as means ± SD, $n = 3$, *$p < 0.05$; **$p < 0.01$; *** $p < 0.001$).

Exosomal MMP1 promotes tumor growth in vivo

A subcutaneous tumorigenesis assay was performed in nude mice. The results showed that the tumor volume in the shCtrl-exo group was the largest compared to the other three groups, and the weight of the subcutaneous tumors was also the heaviest (Fig. 7A–C). Both the injection of exosomes derived from MMP1-knockdown DHLF (shMMP1-exo) and the administration of a PAR1 inhibitor (shCtrl+SCH) effectively mitigated the tumor-promoting effects of DHLF-exo in vivo. Recombinant MMP1 protein also promoted tumor growth, although the effect was less pronounced compared to DHLF-exo. Then, we performed HE staining and IHC staining (Fig. 7D, E). Our IHC results showed that the Ki67 staining intensity was reduced in shMMP1-exo group and shCtrl+SCH group. Western blot analysis was performed to assess the

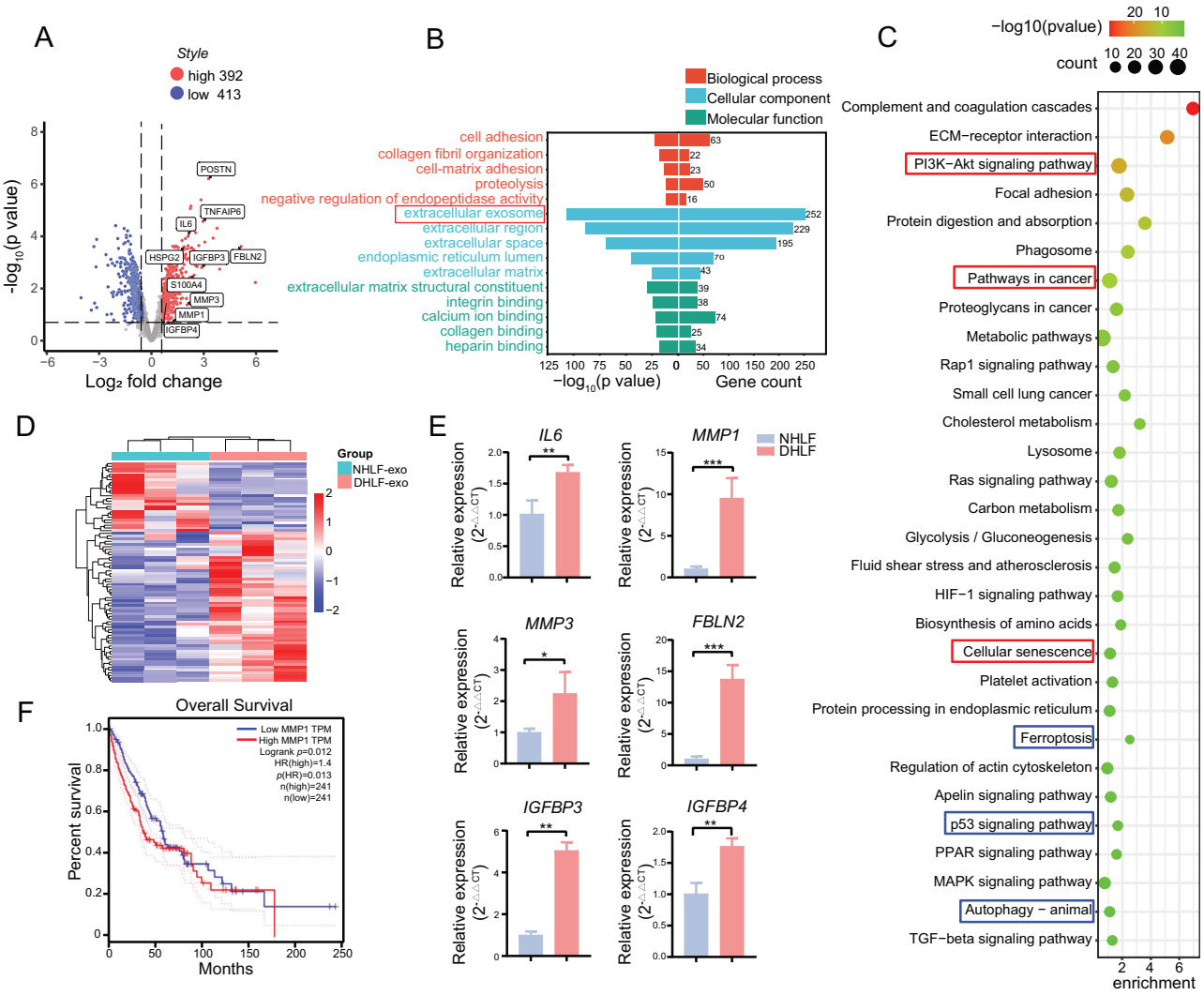

Fig. 4 Mass spectrometry analysis reveals upregulated senescence-associated secretory phenotype (SASP) factors in DHLF-exosomes. **A** Volcano plots illustrating the differential expression of proteins identified by mass spectrometry between exosomes derived from normal human lung fibroblasts (NHLF) and diseased human lung fibroblasts (DHLF). **B** Gene Ontology enrichment analysis of the upregulated proteins, visualized with bar plots. (Top 5 per classification). **C** KEGG pathway enrichment analysis of the top 30 upregulated proteins visualized with a bubble diagram. **D** A heat map showing relative expression levels of SASP factors in NHLF-exosomes and DHLF-exosomes. **E** RT-qPCR analysis of mRNAs encoding SASP factors including *IL-6, MMP1, MMP3, FBLN2, IGFBP3, IGFBP4*. **F** Kaplan–Meier survival analysis curve of low MMP1 and high MMP1 patients derived from 482 patients with NSCLC in TCGA (https://tcga-data.nci.nih.gov/tcga/). TCGA, the cancer genome atlas (Results are presented as means ± SD, $n = 3$, $^{*}p < 0.05$; $^{**}p < 0.01$; *** $p < 0.001$).

activation of PI3K-AKT-mTOR signaling pathway in subcutaneous tumors. The findings demonstrated that p-AKT, p-PI3K, and p-mTOR levels were significantly elevated in the shCtrl-exo group (Fig. 7F, G), suggesting that DHLF-exosomes can effectively activate the PI3K-AKT-mTOR signaling pathway. Therefore, our results validated the pro-tumor effect of exo-MMP1 secreted by DHLF in vivo.

DISCUSSION

Senescence is considered a pivotal pathogenic mechanism in IPF development [23]; although the precise mechanisms of cellular senescence in IPF have not been fully elucidated, they are believed to involve various intrinsic (genetic abnormalities) and extrinsic (oncogene activation and oxidative stress) stressors [24]. Previous studies have demonstrated senescence in the epithelial cells, fibroblasts, and basal cells in IPF samples [15, 25, 26]. Our research confirmed that IPF fibroblasts exhibit senescent characteristics. Extensive research indicates that senescent fibroblasts promote the proliferation of preneoplastic and neoplastic cells and facilitate tumor progression through immunosuppressive mechanisms[12, 27, 28]. By co-culturing senescent lung fibroblasts obtained from IPF samples with NSCLC cells, we demonstrated that these senescent fibroblasts promote NSCLC growth and metastasis.

Senescent cells exert their effects primarily through SASP, which includes cytokines, chemokines, growth factors, and metalloproteinases that promote fibrosis and tumorigenesis. Recently, increasing evidence suggests that SASP is not limited to soluble factors. EVs secreted by senescent cells also exhibit unique characteristics and can transfer their contents (proteins, mRNA, microRNA, and DNA) to exert pro-fibrotic and pro-tumorigenic effects [29]. It is now widely accepted that cellular senescence is associated with increased EV release [29], and s-EVs possess distinct molecular features that contribute to specific functions such as accelerating senescence, as well as

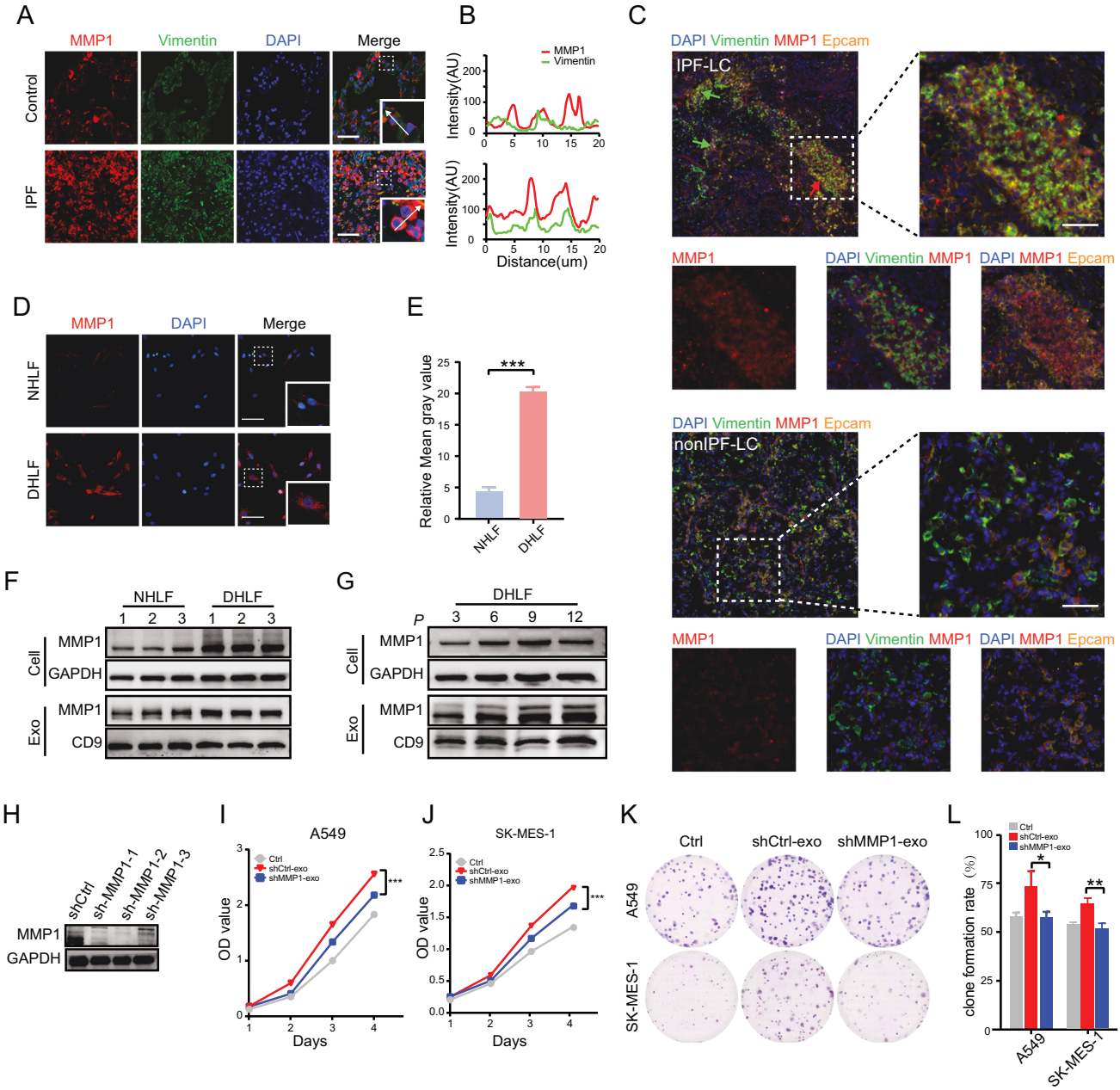

Fig. 5 Upregulation of MMP-1 in IPF-exosomes promotes NSCLC cell proliferation. A, B Double immunofluorescent staining showing MMP1 (red) and Vimentin (green) expression in lung tissue sections. Scale bar, 50 μm. **C** Multiplex immunofluorescence profiling of MMP1 (red) in cancer cells (Epcam, orange) and fibroblasts (Vimentin, green) from interstitial pulmonary fibrosis-lung cancer (IPF-LC) and non-IPF-LC tissues. Scale bar, 50 μm. **D, E** Immunofluorescent staining of MMP-1 expression in primary cells extracted from control and IPF tissues, with representative images and statistical analyses shown in (**D**) and (**E**). Scale bar, 200 μm. **F** Western blot analysis of expression level of MMP-1 in NHLF, DHLF and their corresponding exosomes. **G** Western blot analysis of MMP-1 expressions in NHLF, DHLF, NHLF-exosomes, and NHLF-exosomes at increasing passages. **H** Immunoblot confirming MMP1 knockdown. **I, J** CCK8 assays measuring A549 (**I**) and SK-MES-1 (**J**) cells proliferation incubated with shCtrl-exosomes and shMMP1-exosomes. **K, L** Representative images (**K**) and histogram analysis (**L**) of colony formation incubated with shCtrl-exosomes and shMMP1-exosomes. (Results are presented as means ± SD, $n = 3$, $^{*}p < 0.05$; $^{**}p < 0.01$; $^{***}p < 0.001$).

inducing inflammation, stem cell dysfunction, and cancer progression [16, 17, 30]. Proteomic analysis of exosomes secreted by IPF and normal lung fibroblast cell lines revealed significant differences. The difference in POSTN expression was the most significant. POSTN is overexpressed in various solid tumors and promotes tumor growth and metastasis in cancers such as breast, colon, lung, gastric, pancreatic, ovarian cancer, and melanoma. It facilitates these processes by activating signaling pathways like PI3K/Akt and others [31, 32]. Additional, PAI-1, encoded by *SERPINE1*, acts as an inhibitor of uPA and is an effective mediator of cancer dissemination [33], and it is a key regulator of cancer-associated vascular remodeling [34–36]. *SNRPD1* is also associated with poor prognosis in lung cancer [37]. Additionally, we identified a unique protein expression profile of SASP factors in exosomes derived from IPF fibroblasts. Many of the SASP factors identified in this study are known to

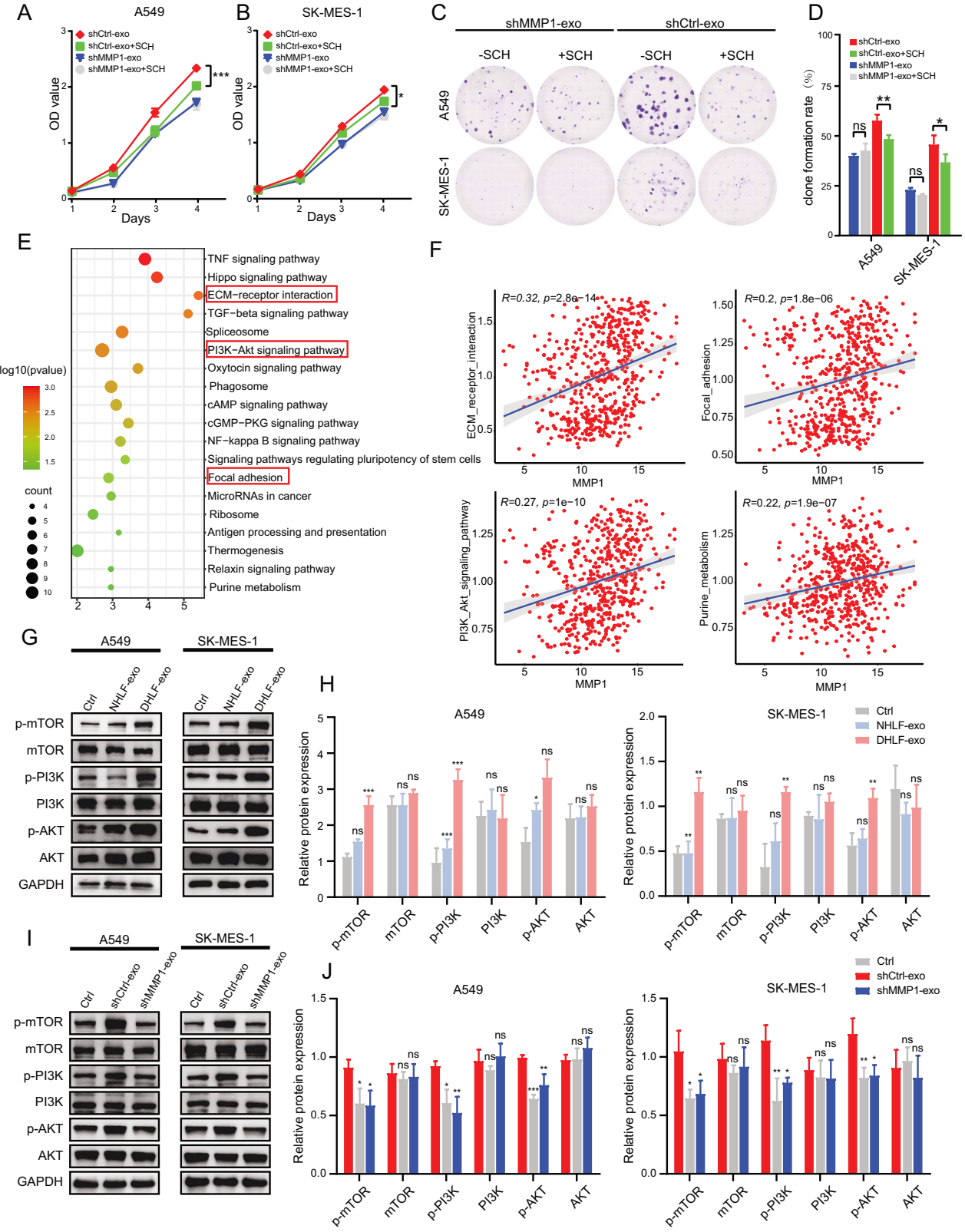

impact the tumor microenvironment. Previous studies have reported that IL-6, produced by various cell types within the tumor microenvironment, activates the JAK/STAT3 signaling pathway in both tumor cells and tumor-infiltrating immune cells, thereby promoting tumor cell proliferation, survival, invasion, and metastasis [38]. Growth factors such as VEGF and HGF promote angiogenesis, providing nutrient supply for tumor growth and enhancing tumor progression and metastasis [39, 40]. Additionally, tumor-associated fibroblasts release various IGFBPs, which regulate cell proliferation, apoptosis, migration, immune responses, and tumor resistance to therapies [41].

Fig. 6 MMP-1 enhances NSCLC cell proliferation by binding with PAR1 and subsequently activating the PI3K-AKT-mTOR signaling pathways. A, **B** CCK8 assays measuring the proliferation of A549 (**A**) and SK-MES-1 cells (**B**) incubated with exosomes isolated from DHLF with MMP1 knockdown (shMMP1) or non-silencing controls (shCtrl) in the presence (+) or absence (–) of a PAR1 antagonist (SCH79797, SCH). **C**, **D** Representative images (**C**) and histogram analysis (**D**) of colony formation of cells incubated with exosomes isolated from shMMP1 or shCtrl fibroblasts in the presence (+) or absence (–) of a PAR1 antagonist (SCH79797, SCH). **E** Bubble chart of KEGG pathway enrichment analysis of 589 candidate differentially expressed genes based on RNA-seq of SK-MES-1 cells incubated without exosome *vs.* SK-MES-1 cells incubated with NHLF-exosome. **F** Analysis of the TCGA database showing the correlation between MMP1 and KEGG enrichment pathway-related genes, with the four strongest correlations highlighted. **G**, **H** Western blot analysis of PI3K-AKT-mTOR pathway activation in A549 and SK-MES-1 cells incubated with NHLF-exosomes, DHLF-exosomes. Band intensities were quantified using ImageJ (**H**). **I**, **J** Western blot analysis of PI3K-AKT-mTOR pathway activation in A549 and SK-MES-1 cells incubated with shCtrl-exosomes and shMMP1-exosomes. Band intensities were quantified using ImageJ (**J**). (Results are presented as means ± SD, $n = 3$, $^{*}p < 0.05$; $^{**}p < 0.01$; $^{***}p < 0.001$).

Our study identified MMP1 as a crucial SASP factor in IPF fibroblasts. MMP1, which degrades collagen, is overexpressed in IPF tissues in our research. We hypothesize that the high expression of MMP1 in IPF fibroblasts is a self-repair mechanism to maintain homeostasis following inflammatory damage. By inducing replicative senescence in fibroblasts, we found increased MMP1 expression, indicating its role as an important SASP factor. Notably, MMP1 is highly expressed in various tumors and is considered a poor prognostic factor. It promotes the progression of esophageal, breast, and prostate cancer. Studies have shown that IL-8 promotes head and neck cancer invasion by activating MMP1 expression in fibroblasts [42]. Consistent with these findings, we confirm that MMP1 is a key factor in promoting NSCLC growth. Our research also revealed that MMP1 exerts its pro-tumor effects by binding to PAR1 and activating the PI3K-AKT-mTOR pathway. Additionally, MMP1-induced senescent fibroblast enhances large-cell lung cancer invasiveness [43], indicating a complex interaction network between MMP1 and fibroblast senescence.

Based on our findings, we propose that fibroblast senescence not only promotes lung fibrosis but also significantly contributes to the progression of IPF-LC, suggesting that targeting senescent fibroblasts could be a novel therapeutic strategy for IPF-LC. This supports the potential of senotherapeutics to inhibit the tumor-promoting effects of senescent fibroblasts [44–46]. With respect to the crucial role of MMP1, targeting MMP1 appears to be another viable therapeutic target. However, many phase III clinical trials using broad-spectrum MMP inhibitors for various cancers have been hampered by dose-limiting joint toxicity [47]. Therefore, targeting the MMP-1 receptor, PAR1, seems a promising alternative, and it had been demonstrated that low concentrations of PAR1 inhibitors can effectively inhibit MMP1-induced lung cancer growth in vivo and in vitro. PAR1 inhibitors are widely utilized in the clinical management of thrombotic cardiovascular diseases [48], with Vorapaxar being the first PAR1 inhibitor approved for clinical use [49]. Moreover, PAR1 inhibitors have demonstrated the capacity to block thrombin-mediated activation of the PAR1 signaling pathway, subsequently inhibiting tumor proliferation, metastasis, angiogenesis, and inflammatory responses [50]. These inhibitors have shown potential therapeutic benefits across various inflammation-associated cancer types [51]. Interestingly, PAR1 inhibitors have also been shown to potentially slow or even reverse the progression of pulmonary fibrosis [52, 53]. Based on these findings, we hypothesize that PAR1 represents a viable therapeutic target for IPF-LC, with PAR1 inhibitors potentially blocking tumor progression and mitigating the severity of pulmonary fibrosis in these patients. One limitation of this study is the exclusive focus on the pro-tumor effects of exosomal MMP1 secreted by IPF fibroblasts, without a comprehensive investigation of the complex roles of other active components within the exosomes. Future research will address this gap by examining the roles of additional factors in the progression and development of IPF-LC, with the aim of identifying more potential therapeutic targets. Another limitation is the relatively small sample size of IPF patients and healthy controls. In future studies, we plan to collect additional specimens to progressively enhance the reliability and validity of our findings.

In summary, this study highlights that senescent fibroblasts in IPF promote NSCLC progression by releasing senescence-associated exosomes carrying MMP1, which activates the PI3K-AKT-MTOR signaling pathway via PAR1 (Fig. 7H). Therefore, targeting senescent fibroblasts or key factors such as MMP1 and PAR1 may be a therapeutic strategy for IPF-LC.

MATERIALS AND METHODS

Cell lines and culture

The lung adenocarcinoma cell line A549 and the lung squamous carcinoma cell line SK-MES-1 were purchased from the cell bank of the Chinese Academy of Sciences (Shanghai, China). Cells were cultured in Dulbecco's Modified Eagle's Medium (DMEM; Gibco) supplemented with 10% fetal bovine serum (FBS; Gibco) and 1% penicillin/streptomycin (100X, Gibco) in an incubator at 37 °C with 5% CO2.

Isolation of primary fibroblasts and co-culture experiment

Lung specimens were obtained from the First Affiliated Hospital of Zhejiang University, and the collection was approved by the Ethics Committee (Institutional Review Board approval no. 2021/330). Informed consent was obtained from all participants before enrollment in the study. Lung tissues from five patients with IPF who underwent lung transplantation were collected as the disease group, and tissues from the distal site of five patients with benign lung nodules were collected as the control group. The patients with IPF met the diagnostic criteria of the American Thoracic Society and the European Respiratory Society. The clinical characteristics of the patients are detailed in Supplementary Table 1. To mitigate the impact of environmental factors, we selected IPF patients and healthy controls from the eastern coastal regions of China ensuring similar living environments, as well as comparable age and smoking history as much as possible. All patients with IPF were administered anti-fibrotic drugs.

Specimens were chopped into small pieces and mixed with collagenase IV (Sigma, USA) for 2 h. The supernatant was filtered through a 70 μm filter, and the centrifuged cells were incubated in DMEM (Gibco) supplemented with 10% fetal bovine serum (FBS) and 1% 100X penicillin/streptomycin. After 72 h, non-adherent cells were discarded, and adherent cells were identified by immunofluorescence (IF). Fibroblasts were passaged to P2–P6 for functional experiments, and both cell lines were kept at the same passage number to exclude the possible influence of replicative senescence on the experiments.

For the co-culture experiments, NSCLC cell lines were seeded uniformly in 6-well plates at a density of 1×10^5 cells per well. Fibroblasts, also seeded at a density of 1×10^5 cells per well, were introduced into the upper chamber of a transwell insert (pore size: 0.4 μm; Costar, USA). Following cell adhesion, the co-cultures were incubated under standard conditions. After 72 h of incubation, the lung cancer cells in the lower chamber were digested with TrypLE and subsequently harvested for further analyses, including the CCK-8 assay, colony formation assay, and Transwell migration and invasion assays, as well as western blot analyses.

CCK8 assay

After co-culture, cocultured A549 and SK-MES-1 cells were inoculated into a 96-well plate at a density of 2×10^3cells/well and 2.5×10^3cells/well,

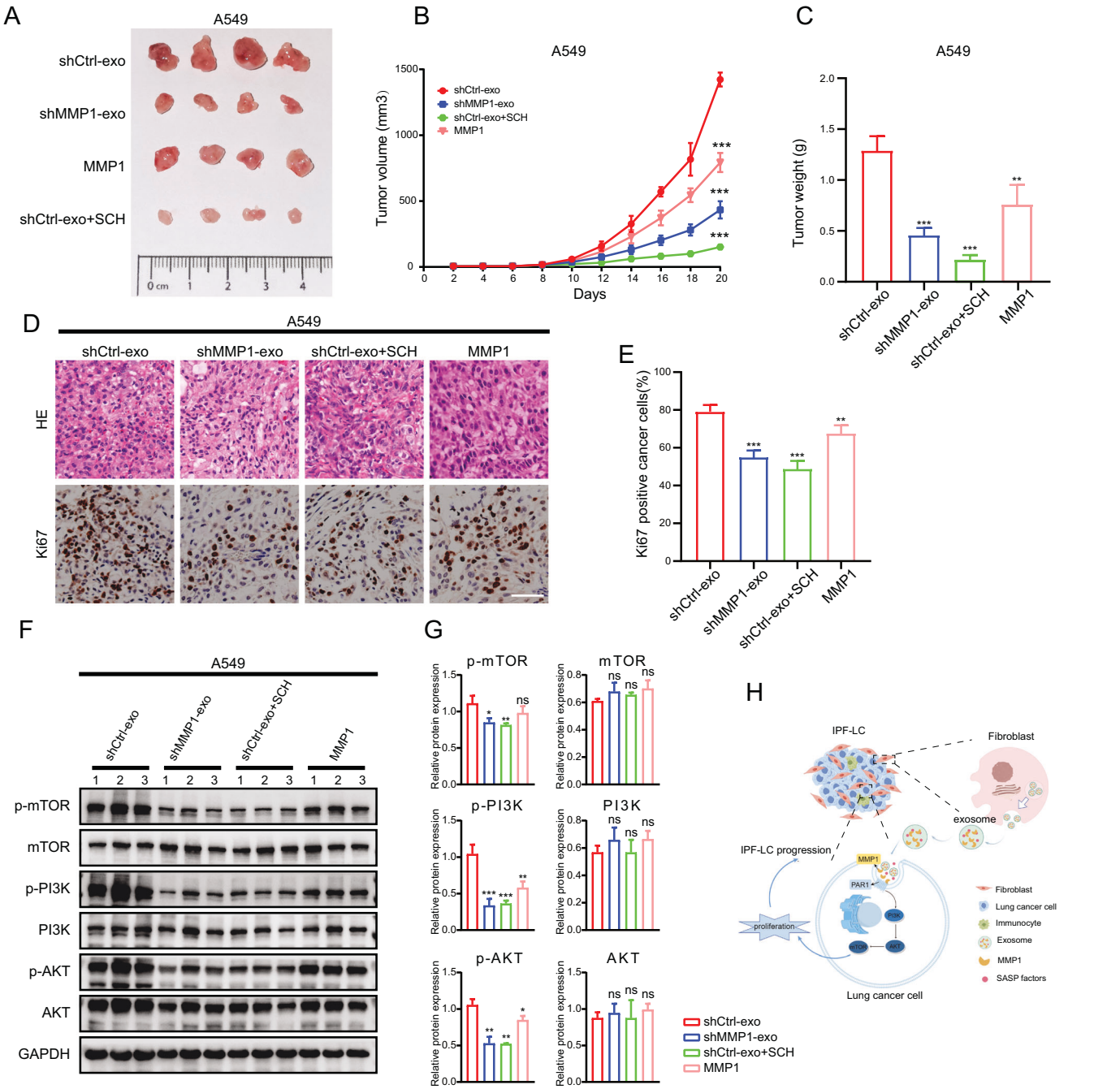

Fig. 7 Exosomal MMP1 promotes tumor growth in vivo. A Xenograft tumors in shCtrl-exo group, shMMP1-exo group, shCtrl-exo+SCH group, and MMP1 group. **B** Tumor growth curves showing the effect of different treatments on A549. **C** Tumor weight comparison across experimental groups after treatment with shCtrl-exo, shMMP1-exo, shCtrl-exo+SCH, and MMP1. **D**, **E** Representative hematoxylin and eosin (H&E) staining and Ki67 immunohistochemical staining of A549 tumor sections from different treatment groups: shCtrl-exo, shMMP1-exo, shCtrl-exo+SCH, and MMP1 (**D**). Quantitative analysis of Ki67-positive cancer cells (%) across treatment groups (**E**). Scale bar, 50 μm. **F**, **G** Western blot analysis of PI3K-AKT-mTOR pathway activation in subcutaneous tumors in mice under different treatment conditions. Representative blot images and corresponding quantitative analyses are shown in (**F**) and (**G**), respectively. **H** Graphical abstract illustrates the role of IPF-derived fibroblast exosomes, particularly exosomal MMP1, in promoting the progression of lung cancer through the PI3K-AKT-mTOR signaling pathway. (Created with Figdraw) (Results are presented as means ± SD, $n = 4$, $^{*}p < 0.05$; $^{**}p < 0.01$; *** $p < 0.001$).

respectively. In the exosome incubation experiments, lung cancer cells were seeded in 96-well plates at a uniform cell density using complete culture medium, and after allowing for cell adhesion, the medium was replaced with fresh medium containing exosomes and/or inhibitor drugs. For the next 3–4 days, CCK8 reagent (Beyotime Biotechnology, Shanghai, China) was added to the wells at the ratio of 1:10 every 24 h and incubated for 2 h at 37 °C. Absorption at 450 nm was measured using a microplate reader (CMax Plus, Shanghai, China).

Clone formation assay

After co-culture, A549 and SK-MES-1 were collected for clone formation assay. Two hundred or one hundred cancer cells were seeded in each well of 6-well or 12-well plates respectively and incubated at 37 °C under 5% CO2 for 10–14 days. In other colony formation assays, untreated lung cancer cells were seeded into well plates, and exosomes and/or inhibitor drugs were added to the culture medium according to the specific experimental conditions. When the clones could be distinguished by the

naked eye, the cells were fixed in 4% paraformaldehyde and stained using a crystal violet staining solution (Sigma-Aldrich, USA). The number of clonies with more than 50 cells was counted under the microscope.

Exosome isolation

Fibroblasts were cultured in a complete medium supplemented with exosome-depleted FBS. When the cells reached 80% confluence, the medium was removed, and the cells were washed three times with PBS. Serum-free medium was then added and the fibroblasts were cultured for another 24 h. Exosomes were isolated from the cell culture supernatant using a differential ultracentrifugation method. The medium was first centrifuged at $300 \times g$ for 10 min, followed by centrifugation at $2000 \times g$ for 10 min to remove cells and cellular debris. Subsequently, the medium was filtered using a 0.22 μm Sterile filter unit (Millipore), and the filter was washed with PBS. The extracellular vesicles (EVs) larger than 0.22 μm retained on the filter were classified as microvesicles (MVs) and resuspended in PBS. The filtered medium was then centrifuged at $15{,}000 \times g$ for 30 min to further pellet MVs, and exosomes were isolated by centrifugation at $150{,}000 \times g$ for 70 min. The resulting pellets were washed once with PBS and resuspended for subsequent experiments. Exosome protein concentration was determined using a BCA protein assay kit (NCM Biotech, China). Exosome characterization was performed using a transmission electron microscope (TEM) for morphology, a nanoparticle tracking analyzer (NTA) for particle size analysis, and western blotting (WB) for signature protein identification.

Statistical analysis

All experiments were conducted at least in triplicate, and results are expressed as mean ± standard deviation. Statistical analyses were performed using GraphPad Prism 8.0. Independent samples t test was utilized to compare differences between the two groups. One-way ANOVA with Tukey's multiple comparisons test was used for the analysis involving three or more groups. Statistical significance was determined by $^{*}p < 0.05$, $^{**}p < 0.01$, and $^{***}p < 0.001$.

DATA AVAILABILITY

Materials described in the manuscript, including all relevant raw data, will be freely available to any scientist wishing to use them for non-commercial purposes. The proteomics data have been deposited in the Figshare repository (https://doi.org/10.6084/m9.figshare.26233301). RNA-seq data have been deposited in the GEO repository (GSE279637).

REFERENCES

1. Tzouvelekis A, Antoniou K, Kreuter M, Evison M, Blum TG, Poletti V, et al. The DIAMORFOSIS (DIAgnosis and Management Of lung canceR and FibrOSIS) survey: international survey and call for consensus. ERJ Open Res. 2021;7:00529–2020.
2. Tomassetti S, Gurioli C, Ryu JH, Decker PA, Ravaglia C, Tantalocco P, et al. The impact of lung cancer on survival of idiopathic pulmonary fibrosis. Chest. 2015;147:157–64.
3. Raghu G, Amatto VC, Behr J, Stowasser S. Comorbidities in idiopathic pulmonary fibrosis patients: a systematic literature review. Eur Respir J. 2015;46:1113–30.
4. Fujimoto D, Morimoto T, Ito J, Sato Y, Ito M, Teraoka S, et al. A pilot trial of nivolumab treatment for advanced non-small cell lung cancer patients with mild idiopathic interstitial pneumonia. Lung Cancer. 2017;111:1–5.
5. Fujimoto D, Yomota M, Sekine A, Morita M, Morimoto T, Hosomi Y, et al. Nivolumab for advanced non-small cell lung cancer patients with mild idiopathic interstitial pneumonia: A multicenter, open-label single-arm phase II trial. Lung Cancer. 2019;134:274–8.
6. Zhang H, Jiang H, Zhu L, Li J, Ma S. Cancer-associated fibroblasts in non-small cell lung cancer: Recent advances and future perspectives. Cancer Lett. 2021;514:38–47.
7. Samarelli AV, Masciale V, Aramini B, Coló GP, Tonelli R, Marchioni A, et al. Molecular mechanisms and cellular contribution from lung fibrosis to lung cancer development. Int J Mol Sci. 2021;22:12179.
8. Yamato H, Kimura K, Fukui E, Kanou T, Ose N, Funaki S, et al. Periostin secreted by activated fibroblasts in idiopathic pulmonary fibrosis promotes tumorigenesis of non-small cell lung cancer. Sci Rep. 2021;11:21114.
9. Chen T, Guo J, Ai L, Wang Y, Wang Y, Chen B, et al. Up-regulated SPP1 increases the risk from IPF to lung cancer via activating the pro-tumor macrophages. Comput Struct Biotechnol J. 2023;21:5751–64.
10. Faner R, Rojas M, Macnee W, Agustí A. Abnormal lung aging in chronic obstructive pulmonary disease and idiopathic pulmonary fibrosis. Am J Respir Crit Care Med. 2012;186:306–13.
11. Sun Y, Coppé JP, Lam EW. Cellular senescence: the sought or the unwanted? Trends Mol Med. 2018;24:871–85.
12. Krtolica A, Parrinello S, Lockett S, Desprez PY, Campisi J. Senescent fibroblasts promote epithelial cell growth and tumorigenesis: a link between cancer and aging. Proc Natl Acad Sci USA. 2001;98:12072–7.
13. Bavik C, Coleman I, Dean JP, Knudsen B, Plymate S, Nelson PS. The gene expression program of prostate fibroblast senescence modulates neoplastic epithelial cell proliferation through paracrine mechanisms. Cancer Res. 2006;66:794–802.
14. Roninson IB. Oncogenic functions of tumour suppressor p21(Waf1/Cip1/Sdi1): association with cell senescence and tumour-promoting activities of stromal fibroblasts. Cancer Lett. 2002;179:1–14.
15. Yanai H, Shteinberg A, Porat Z, Budovsky A, Braiman A, Zeische R, et al. Cellular senescence-like features of lung fibroblasts derived from idiopathic pulmonary fibrosis patients. Aging (Albany NY). 2015;7:664–72.
16. Weilner S, Schraml E, Wieser M, Messner P, Schneider K, Wassermann K, et al. Secreted microvesicular miR-31 inhibits osteogenic differentiation of mesenchymal stem cells. Aging Cell. 2016;15:744–54.
17. Takasugi M, Okada R, Takahashi A, Virya Chen D, Watanabe S, Hara E. Small extracellular vesicles secreted from senescent cells promote cancer cell proliferation through EphA2. Nat Commun. 2017;8:15729.
18. Saul D, Kosinsky RL, Atkinson EJ, Doolittle ML, Zhang X, LeBrasseur NK, et al. A new gene set identifies senescent cells and predicts senescence-associated pathways across tissues. Nat Commun. 2022;13:4827.
19. Baege AC, Disbrow GL, Schlegel R. IGFBP-3, a marker of cellular senescence, is overexpressed in human papillomavirus-immortalized cervical cells and enhances IGF-1-induced mitogenesis. J Virol. 2004;78:5720–7.
20. Mao S, Xia A, Tao X, Ye D, Qu J, Sun M, et al. A pan-cancer analysis of the prognostic and immunological roles of matrix metalloprotease-1 (MMP1) in human tumors. Front Oncol. 2022;12:1089550.
21. Huang C, Li Y, Guo Y, Zhang Z, Lian G, Chen Y, et al. MMP1/PAR1/SP/NK1R paracrine loop modulates early perineural invasion of pancreatic cancer cells. Theranostics. 2018;8:3074–86.
22. Boire A, Covic L, Agarwal A, Jacques S, Sherifi S, Kuliopulos A. PAR1 is a matrix metalloprotease-1 receptor that promotes invasion and tumorigenesis of breast cancer cells. Cell. 2005;120:303–13.
23. Schafer MJ, White TA, Iijima K, Haak AJ, Ligresti G, Atkinson EJ, et al. Cellular senescence mediates fibrotic pulmonary disease. Nat Commun. 2017;8:14532.
24. Parimon T, Hohmann MS, Yao C. Cellular senescence: pathogenic mechanisms in lung fibrosis. Int J Mol Sci. 2021;22:6214.
25. Álvarez D, Cárdenes N, Sellarés J, Bueno M, Corey C, Hanumanthu VS, et al. IPF lung fibroblasts have a senescent phenotype. Am J Physiol Lung Cell Mol Physiol. 2017;313:L1164–73.
26. Ramos C, Montaño M, García-Alvarez J, Ruiz V, Uhal BD, Selman M, et al. Fibroblasts from idiopathic pulmonary fibrosis and normal lungs differ in growth rate, apoptosis, and tissue inhibitor of metalloproteinases expression. Am J Respir Cell Mol Biol. 2001;24:591–8.
27. Ye J, Baer JM, Faget DV, Morikis VA, Ren Q, Melam A, et al. Senescent CAFs mediate immunosuppression and drive breast cancer progression. Cancer Discov. 2024;14:1302–23.
28. Freeland J, Crowell PD, Giafaglione JM, Boutros PC, Goldstein AS. Aging of the progenitor cells that initiate prostate cancer. Cancer Lett. 2021;515:28–35.
29. Kadota T, Fujita Y, Yoshioka Y, Araya J, Kuwano K, Ochiya T. Emerging role of extracellular vesicles as a senescence-associated secretory phenotype: Insights into the pathophysiology of lung diseases. Mol Asp Med. 2018;60:92–103.
30. Davis C, Dukes A, Drewry M, Helwa I, Johnson MH, Isales CM, et al. MicroRNA-183-5p increases with age in bone-derived extracellular vesicles, suppresses bone marrow stromal (stem) cell proliferation, and induces stem cell senescence. Tissue Eng Part A. 2017;23:1231–40.
31. Ruan K, Bao S, Ouyang G. The multifaceted role of periostin in tumorigenesis. Cell Mol Life Sci. 2009;66:2219–30.
32. Cui D, Huang Z, Liu Y, Ouyang G. The multifaceted role of periostin in priming the tumor microenvironments for tumor progression. Cell Mol Life Sci. 2017;74:4287–91.
33. Li S, Wei X, He J, Tian X, Yuan S, Sun L. Plasminogen activator inhibitor-1 in cancer research. Biomed Pharmacother. 2018;105:83–94.
34. Fox SB, Taylor M, Grøndahl-Hansen J, Kakolyris S, Gatter KC, Harris AL. Plasminogen activator inhibitor-1 as a measure of vascular remodelling in breast cancer. J Pathol. 2001;195:236–43.
35. Offersen BV, Pfeiffer P, Andreasen P, Overgaard J. Urokinase plasminogen activator and plasminogen activator inhibitor type-1 in nonsmall-cell lung cancer: relation to prognosis and angiogenesis. Lung Cancer. 2007;56:43–50.
36. Isogai C, Laug WE, Shimada H, Declerck PJ, Stins MF, Durden DL, et al. Plasminogen activator inhibitor-1 promotes angiogenesis by stimulating endothelial cell migration toward fibronectin. Cancer Res. 2001;61:5587–94.

37. Duan G, Huang C, Zhao J, Zhang Y, Zhao W, Dai H. Investigating subtypes of lung adenocarcinoma by oxidative stress and immunotherapy related genes. Sci Rep. 2023;13:20930.
38. Johnson DE, O'Keefe RA, Grandis JR. Targeting the IL-6/JAK/STAT3 signalling axis in cancer. Nat Rev Clin Oncol. 2018;15:234–48.
39. Ferrara N, Gerber HP, LeCouter J. The biology of VEGF and its receptors. Nat Med. 2003;9:669–76.
40. Gherardi E, Birchmeier W, Birchmeier C, Woude Vande. G. Targeting MET in cancer: rationale and progress. Nat Rev Cancer. 2012;12:89–103.
41. Remsing Rix LL, Sumi NJ, Hu Q, Desai B, Bryant AT, Li X, et al. IGF-binding proteins secreted by cancer-associated fibroblasts induce context-dependent drug sensitization of lung cancer cells. Sci Signal. 2022;15:eabj5879.
42. Chen Y, Huang L, Gan RH, Yuan S, Lan T, Zheng D, et al. IL-8 activates fibroblasts to promote the invasion of HNSCC cells via STAT3-MMP1. Cell Death Discov. 2024;10:65.
43. Gabasa M, Radisky ES, Ikemori R, Bertolini G, Arshakyan M, Hockla A, et al. MMP1 drives tumor progression in large cell carcinoma of the lung through fibroblast senescence. Cancer Lett. 2021;507:1–12.
44. Muñoz-Espín D, Serrano M. Cellular senescence: from physiology to pathology. Nat Rev Mol Cell Biol. 2014;15:482–96.
45. Zhang L, Pitcher LE, Prahalad V, Niedernhofer LJ, Robbins PD. Targeting cellular senescence with senotherapeutics: senolytics and senomorphics. Febs j. 2023;290:1362–83.
46. Justice JN, Nambiar AM, Tchkonia T, LeBrasseur NK, Pascual R, Hashmi SK, et al. Senolytics in idiopathic pulmonary fibrosis: Results from a first-in-human, open-label, pilot study. EBioMedicine. 2019;40:554–63.
47. Yamamoto A, Yano S, Shiraga M, Ogawa H, Goto H, Miki T, et al. A third-generation matrix metalloproteinase (MMP) inhibitor (ONO-4817) combined with docetaxel suppresses progression of lung micrometastasis of MMP-expressing tumor cells in nude mice. Int J Cancer. 2003;103:822–8.
48. Lee S. Discovery of an orally available PAR-1 antagonist as a novel antiplatelet agent. Arch Pharm Res. 2011;34:515–7.
49. Poole RM, Elkinson S. Vorapaxar: first global approval. Drugs. 2014;74:1153–63.
50. Nierodzik ML, Karpatkin S. Thrombin induces tumor growth, metastasis, and angiogenesis: evidence for a thrombin-regulated dormant tumor phenotype. Cancer Cell. 2006;10:355–62.
51. Li X, Kurahara LH, Zhao Z, Zhao F, Ishikawa R, Ohmichi K, et al. Therapeutic effect of proteinase-activated receptor-1 antagonist on colitis-associated carcinogenesis. Cell Mol Gastroenterol Hepatol. 2024;18:105–31.
52. Lin C, Borensztajn K, Spek CA. Targeting coagulation factor receptors - protease-activated receptors in idiopathic pulmonary fibrosis. J Thromb Haemost. 2017;15:597–607.
53. Lin C, Duitman J, Daalhuisen J, Ten Brink M, von der Thüsen J, van der Poll T, et al. Targeting protease activated receptor-1 with P1pal-12 limits bleomycin-induced pulmonary fibrosis. Thorax. 2014;69:152–60.

ACKNOWLEDGEMENTS

We thank Figdraw as the flowchart and schematic diagram in this article were drawn by Figdraw.

AUTHOR CONTRIBUTIONS

TR and CWH conceived and supervised the project. ZBL provided and validated the lung transplant specimens from IPF patients, and facilitated clinical translation of our findings. YQL designed the experiments. YQL, CZ, JYZ conducted experiments and analyzed data. QZ, YLX, ZBL provided access to material and facilities and contributed reagents. YQL writed original draft. TR and CWH edited the manuscript. All the authors reviewed and approved the final manuscript.

FUNDING

This work was supported by the National Natural Science Foundation of China (81930001), Medicine and Engineering Interdisciplinary Research Fund of Shanghai Jiao Tong University (YG2020YQ18, ZH2018ZDA21), Shanghai Leading Talent Plan (2020, 064).

COMPETING INTERESTS

The authors declare no competing interests.

INFORMED CONSENT STATEMENT

Informed consent was obtained from all participants involved in this study. The study received approval from the Ethics Committee of First Affiliated Hospital of Zhejiang University (Institutional Review Board approval no. 2021/330).

ADDITIONAL INFORMATION

Supplementary information The online version contains supplementary material available at https://doi.org/10.1038/s41388-024-03236-5.

Correspondence and requests for materials should be addressed to Zhoubin Li, Chenwen Huang or Tao Ren.